Application of Shuttle Imaging Radar Data for Land Use Investigations

LIU JIYUAN

Institute of Remote Sensing Application, Academia Sinica, Beijing, China

TENG XUYAN

Changchun Institute of Physics, Academia Sinica, Changchun, Jilin, China

XIAO JINKAI

Institute of Geochemistry, Academia Sinica, Guiyang, Guizhou, China

A Shuttle Imaging Radar (SIR)-A image in the south of Tianjin acquired by the SIR-A in November 1981 was interpreted manually and with the aid of a computer system. The methods of processing involved density slicing with statistical training, producing normalized false color composite images through coregistration of the SIR-A and Landsat MSS image data sets, and unsupervised clustering. The interpretation keys for the SIR-A image were established after investigation *in situ* and analysis of soil dielectric and moisture properties. The interpretation accuracy for various images was determined by using a combination of color infrared aerial photography and land use maps acquired recently. The research indicates that the SIR-A data can remedy some defects of Landsat MSS data due to the SIR-A's better response to residential areas and linear features. The SIR-A/Landsat MSS normalized composite image incorporated the strong points of both. The interpretation accuracy, therefore was increased.

Introduction

The first shuttle-based radar images with high resolution were acquired by the Shuttle Imaging Radar (SIR)-A which was on the Space Shuttle Columbia in November 1981 (Elachi, et al., 1982). Other investigators have obtained some important results from the SIR-A images in the past several years. For example, they revealed previously unknown buried valleys and other geologic structures under the drift sand of the eastern Sahara (McCauley, et al., 1982). In November 1983, the feasibility of using SIR-A images for land use investigation were studied in combination with investigating the land resource of Tianjin areas. The test site was selected at Tangguantun, county Jinghai, Tianjin. The original SIR-A image in the south of Tianjin is shown in Fig. 1, in which the test site is indicated by the white frame which covers an area 20.5× 20.5 km. The test site is located in the alluvial plain of the western part of the Bohai Bay with smooth terrain and landform features of a typical agricultural area in north China.

The Dependence of the SIR-A Image Greyscale on the Soil Dielectric Properties and Surface Characteristics

By *in situ* investigation, the investigators found that the distribution of crops and the condition of irrigation at the test site were similar in recent years. The same season, in which the SIR-A acquired

©Elsevier Science Publishing Co., Inc., 1986
52 Vanderbilt Ave., New York, NY 10017

0034-4257/86/$3.50

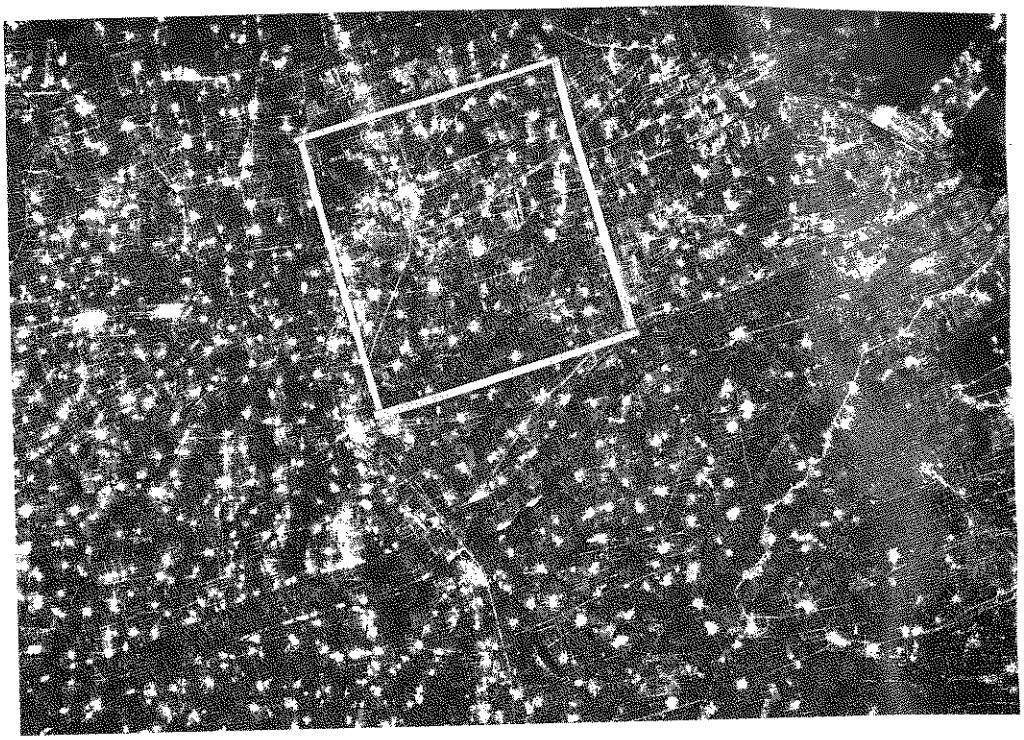

FIGURE 1. The original SIR-A image in the south of Tianjin.

the radar images around the world, was chosen for the field investigation and sampling. The complex dielectric constant of soil samples and soil moisture were measured, and the greyscale values of the SIR-A image corresponding to the areas sampled were also measured by a reflective densitometer (the value of reference standard white plate is 5.90 and the value of black plate is 4.28). The data measured from six areas are listed in Table 1; five to ten samples were taken in

TABLE 1 The Complex Dielectric Constant of Soil Samples, Soil Moisture and the Greyscale Values of the SIR-A Image

The Number of Soil Samples	Types of Landcover	Complex dielectric Constant ε'	Complex dielectric Constant ε''	Soil Moisture Ms (vol. %)	Greyscale Value G
Tj-1	cropland covered by winter wheat	4.30	0.155	15.35	5.28
Tj-2	harvested cropland	3.29	0.131	9.74	4.83
Tj-3	harvested cropland	3.61	0.142	12.24	5.24
Tj-4	harvested cropland	3.45	0.139	10.83	5.02
Tj-5	cropland with salinized soil	3.59	0.149	11.52	5.10
Tj-6	cropland covered by winter wheat	4.19	0.147	14.26	5.43

each area, and the data in Table 1 are on the average. Figure 2 shows some of the sampled areas.

The experiment demonstrated that there exists an evident plus correlativity between the greyscale value of the SIR-A image G and both the complex dielectric constant of soil (real part ϵ' and imaginary part ϵ'') and soil moisture M_s; the corresponding regression equations are

$$G = 3.4446 + 0.4582\epsilon', \quad (1a)$$

$$G = 2.4391 + 18.8474\epsilon'', \quad (1b)$$

$$G = 4.0589 + 8.8537M_s. \quad (1c)$$

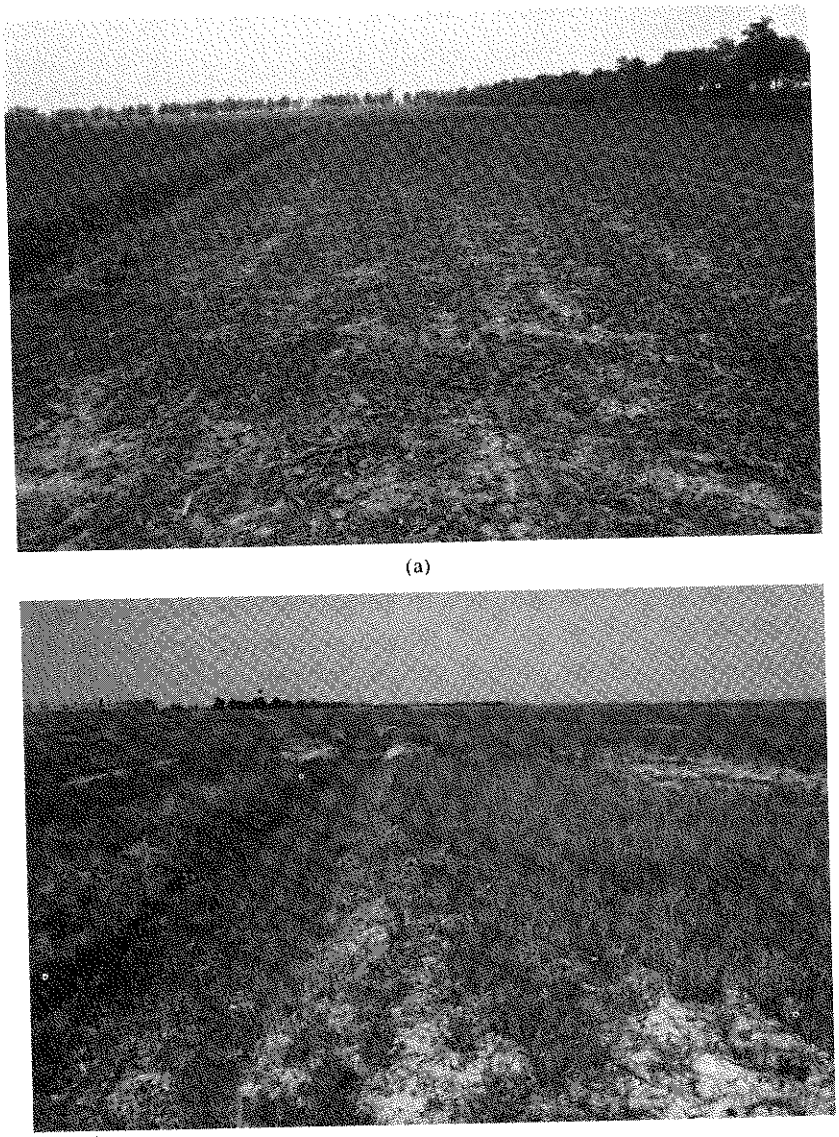

(a)

(b)

FIGURE 2. Photographs taken *in situ* (Nov. 1983, Jinghai, Tianjin): (a) harvested cropland (Tj-3); (b) cropland with salinized soil (Tj-5); (c) cropland covered by winter wheat (Tj-6).

acteristic.
acterized
surface is
According
roughness
(1970), if

acteristic. A rough surface is characterized by bright tones, and a smooth surface is characterized by dark tones. According to the criterion of surface roughness defined by Peake and Oliver (1970), if the height of surface h is

$$h_1 < \frac{\lambda}{25\cos\theta}, \qquad (3a)$$

the surface is smooth; if

$$h_2 > \frac{\lambda}{4.4\cos\theta}, \qquad (3b)$$

the surface is rough. Here λ = the wavelength of radar and θ = the incident angle of radar beam. For the SIR-A, λ = 23 cm, $\theta = 50 \pm 3°$; so, $h_1 = 1.4$ cm and $H_2 = 8.0$ cm. As a result, most of the farmlands in the test site are moderately rough; however, trees, canals, and roads appear to be a fully rough (the Peake and Oliver roughness criterion do not apply to volume scattering objects such as trees). The canal systems that had similar surface roughnesses displayed different tones in the SIR-A image because the intersection angles between the run of these canals and the direction of the radar beam are not alike. Particularly, when a canal's slope becomes a surface facing the radar head-on (the intersection angle is 90°), one can see a bright line on the SIR-A image. The residential areas strongly backscatter the radar signals either because the walls of buildings form corner reflectors with the surface or because of the abundance of metallic structures, or both. Being very bright and irregular, scattered all over like stars in the sky, the residential areas on the image are one of the obvious features in the SIR-A image.

The SIR-A Image Interpretation Key to Land Use Types

The nine typical types of land use at the test site were classified and verified *in situ*. The SIR-A image interpretation keys for land use classification were established as shown in Table 2.

The SIR-A Image Processing by Computer

With the I^{2}S 101 Image Processing System and a density slicing program with statistical training, the investigators processed the SIR-A image. Figure 4 is the SIR-A black and white image of the test site after accurate geometric correction. Figure 5 is the SIR-A color density slice image with five levels. After these, coregistered SIR-A and Landsat MSS data sets were studied extensively. A topographic map (scale is 1:100,000) was used as a control base with a pixel size of 40 m. Seven targets were selected as control points in both images and the map, respectively. These control points formed a triangle control grid. The pixel position of each control point was read respectively. The control points of both images were regarded as input pixels, respectively, the control point of map was regarded as output pixels, and finally, the accurate geometric correction to the both images were achieved through a warp program. Then, the pixels of the both images were made to correspond one by one on the new coordinate grid, the coregistration of the SIR-A image with Landsat MSS image was accomplished. Several programs of image processing within 512×512 pixels were used further; e.g., Landsat MSS (4,

TABLE 2 The SIR-A Image Interpretation Keys for Land Use Types in Tangguantun

Types	The Interpretation Key	Explanation
Dry land	appears as a stretch of dark tones with large areas and uniform texture	The dielectric constant of soil is lower due to dryness and the surface roughness has no serious effect on the image due to flatness and the absence of crops cover
Irrigated land	appears as a medium tone on the dark side image, in which there are large numbers of white and thin lines	The dielectric constant of soil is higher than that of dry land because of moist soil and a covering of winter-wheat seedling. Many small gutters were dispread over the irrigated land
Vegetable plot	similar to the irrigated land and often difficult to distinguish alone	The soil is very damp. Many small gutters and the ridges of vegetable bed are dispersed over the vegetable plot
Orchard	appears as a rectangle bright white tone image and the shapes are generally regular; sometimes it may be confused with residential areas	The surface roughness is very high due to fruit trees and it produces strongly returned echo. Also, being a volume scatterer, the orchard presents a greater density of plant interfaces for reflecting than does a simple rough surface
Pond	it appears as a deep dark tone spot with uniform smooth texture; sometimes, it is similar to a small dry plot	Low returns are received from water surfaces which act as specular reflectors
River and Canals	a bright line or a dark belt sandwiched between the two of bright lines on the image	The earth-filled dams or shelter belts which lie both side of rivers and canals produce strong returned echo. If water surface or flood land is wider than the sensor resolution (40 m), the pattern, in which a dark belt is sandwiched between the two of bright lines, is formed
Highway	a bright line on the image and may be confused with canals, but it can be distinguished on the basis of its relative positions	The shelterbelt which lie on both sides of the highway are so crowded together that they produce strong returned echo.
Railway and transmission towers	brightest for the railway and a row of bright dots keeping an equal distance each other for the transmission towers	The metallic structures are excellent reflectors for electromagnetic wave. The surface along the railway line is very rough
Residential areas	there are many bright and irregular "sparkles" spots on the image	A particularly bright response results from a corner reflector, in this case, adjacent smooth surfaces, i.e., the wall and ground, cause a double reflection that yields a very high return. Otherwise, there are many trees around the towns and villages

5, 7 bands) standard false color composite, standard false color composite using SIR-A image instead of MSS 5 band, producing three new greyscale images through a normalized processing to the SIR-A image and MSS 4, 5, and 7 band images, respectively, as expressed in Eq. (4). Then, conducting the normalized false color composite,

$$N_1 = \frac{M_4 \cdot S}{M_4 \cdot S + M_5 \cdot S + M_7 \cdot S}, \quad (4a)$$

$$N_2 = \frac{M_5 \cdot S}{M_4 \cdot S + M_5 \cdot S + M_7 \cdot S}, \quad (4b)$$

$$N_3 = \frac{M_7 \cdot S}{M_4 \cdot S + M_5 \cdot S + M_7 \cdot S}, \quad (4c)$$

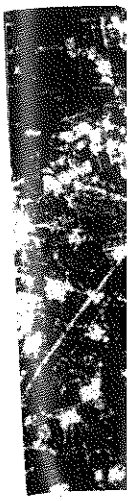

FIGURE 4.
tan, Tianjin,

FIGU

where
4, 5, a
represe
N_3 re
images,
that th
represe
dition,
process

FIGURE 4. SIR-A black and white image (Tangguantun, Tianjin, Nov. 1981).

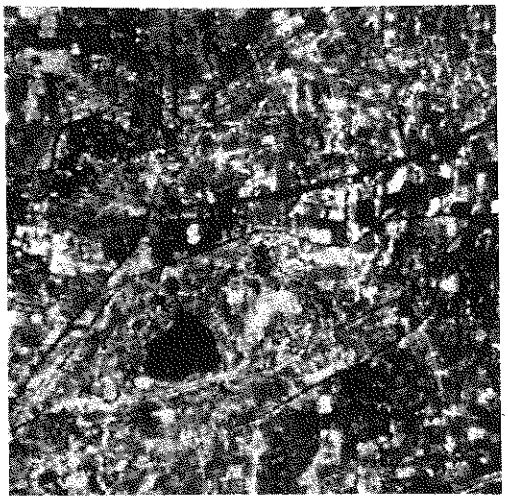

FIGURE 6. Landsat MSS standard composite image processed by the method of Histogram Equiprobable (originally in color).

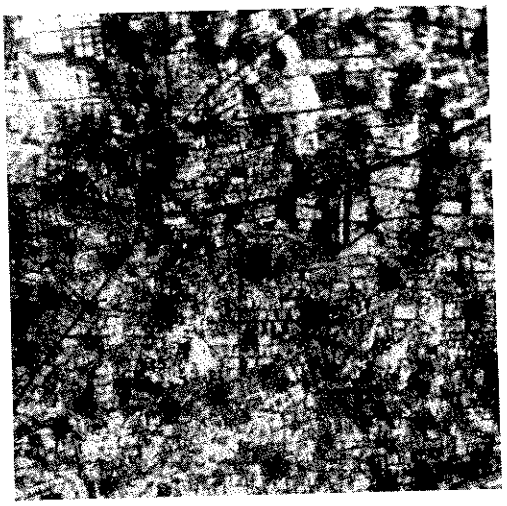

FIGURE 8. SIR-A/Landsat MSS 4, 5, 7 band normalized color composite image (originally in color).

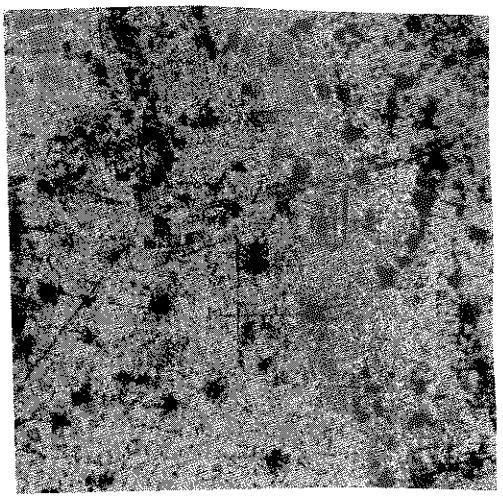

FIGURE 9. Cluster classification result of Fig. 8 (originally in color).

various images (see Figs. 7 and 9). The results indicated that the normalized color composite image can classify six types effectively, involving dry land (sky blue), irrigated land (pink, yellow and blue, criss crossed), vegetable plot (green), reed marshes (pink, with large area), residential area (purplish red), and linear features (purple and cyan line). This image is in an advantageous position for both classifications effect and resolution compared with MSS false color composite image and SIR-A color density slice image.

The Effects of Land Use Interpretation and Accuracy Analysis for Various Images

On the basis of various images, the land use interpretation map (1:100,000) of a part of the test site, surrounding Tangguantun town, had been done respectively to compare their effects to land use direct interpretation. The accuracy analysis of three interpretation maps were conducted according to 208 sampling points selected evenly in the grid and compared with large scale color IR aerial photography (1:50,000) and land use maps acquired recently. Figure 10 illustrates the land use interpretation mapping. The analysis results of three images are given in Table 3.

Obviously, it is impossible or difficult to distinguish the orchards, ponds, and residential areas on the Landsat MSS standard false color composite image (Fig. 6), and the interpretation results for dry land, vegetable plots, rivers, and canals are not good. Especially, many small branch canals cannot be seen due to poor spatial resolution. Similarly, it is also impossible or difficult to distinguish the orchards, ponds, and vegetable plots on the SIR-A density sliced false color image (Fig. 5), and the classification accuracy of residential area is not high because the irregular spots of residential areas on the radar image causes some mistaken interpretation. On the SIR-A/Landsat MSS normalized composite image (Fig. 8),

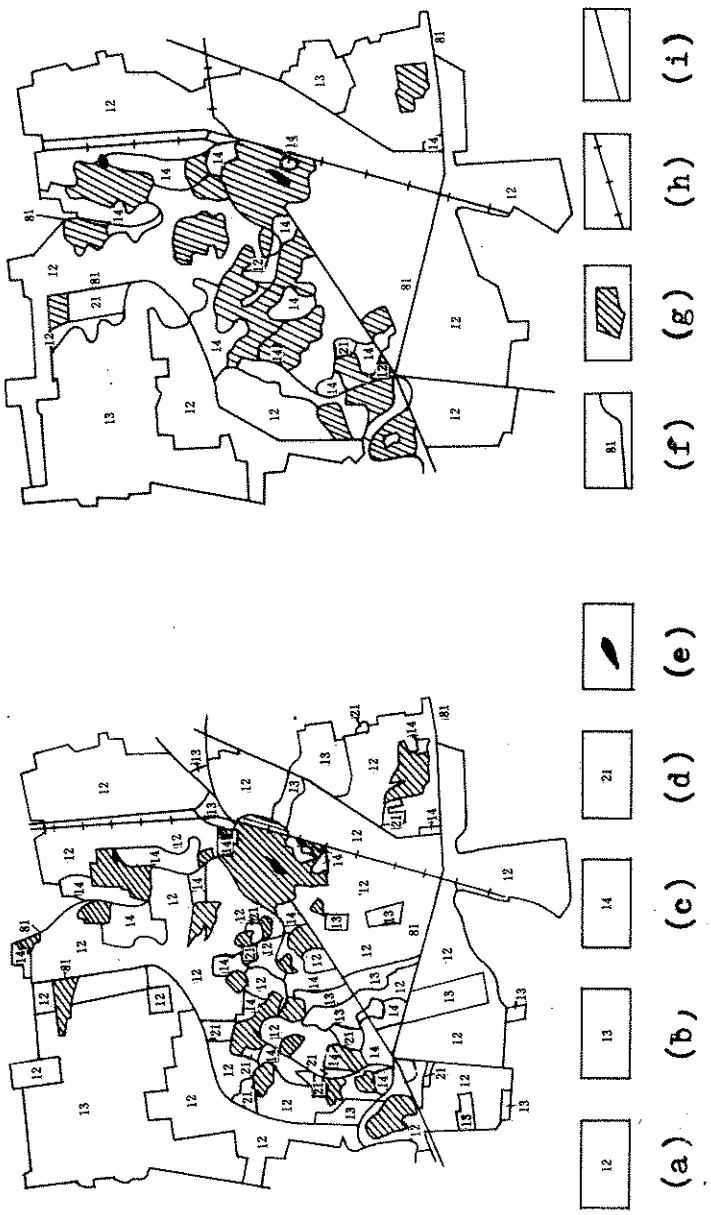

FIGURE 10. The land use interpretation map (1:120,000) on the basis of (a) color IR serial photography and (b) the SIR-A/Landsat MSS normalized color composite image. Legend: (a) irrigated land; (b) dry land; (c) vegetable plot; (d) orchard; (e) pond; (f) river and canals; (g) residential area; (h) railway; (i) highway.

TABLE 3 The Classification Accuracy of Land Use Interpretation for Three Images

Image \ Types — Accuracy (%)	Dry Land	Irrigated Land	Vegetable Plot	Orchard	Pond	River and Canals	Highway	Railway	Residential Areas	Total Accuracy
Landsat MSS standard false color composite image	47.8	67.1	50.0	0.0	0.0	50.0	100.0	100.0	36.4	73.6
SIR-A density slicing image	58.2	66.0	23.5	0.0	0.0	70.0	83.3	80.0	50.0	74.0
SIR-A/Landsat MSS normalized false color composite image	75.0	75.2	45.8	33.3	100.0	71.4	66.7	80.0	59.4	81.7

however, the classification accuracy is higher except for orchard and vegetable plot. This normalized composite image retains not only the spectral reflectance characteristics in the bands of visible and near infrared, but also the backscatter characteristics in the microwave band. In addition, it has both higher resolution and sidelighted features from the SIR-A image. The information content of this image, therefore, is increased considerably in comparison with MSS and SIR-A images. The classification accuracy is increased from 73.6% and 74.0% to 81.7%.

Conclusions

In short, the SIR-A image has both higher resolution and side-lighted features, and it can remedy some defects of Landsat MSS data, especially, showing residential areas and linear features clearly. The digital image processing methods mentioned above, i.e., the coregistration of the Landsat MSS images and the SIR-A images as well as the normalized composite, provide a valuable illustration about the feasibility of using the SIR-A images for land use investigation.

The authors wish to express their sincere thanks to Dr. Kaew Nualchawee, Dr. G. E. Johnson, and Dr. W. M. Hodson, of Asian Regional Remote Sensing Training Center, Asian Institute of Technology, who presented the CCT data recording SIR-A image (north China, in November 1981) to us. We are also grateful to Professor Chen Shupeng, of the Institute of Remote Sensing Application, Academia Sinica, and Associate Professor Zhang Junrong, of the Changchun Institute of Physics, Academia Sinica, whose numerous suggestions were extremely valuable for our research work.

References

Elachi, C., et al. (1982), Shuttle imaging radar experiment, *Science* 218:996–1003.

McCauley, J. F., et al. (1982), Subsurface valleys and geoarcheology of the eastern Sahara revealed by shuttle radar, *Science* 218:1004–1020.

Peake, W. H., and Oliver, T. L., (1970), The response of terrestrial surfaces at microwave frequencies, U.S. Air Force Avionics Lab. Rep. AFAL-TR-70-301.

Received 14 March 1985; revised 28 August 1985.